

Experimental evidence of paired hole states in model high- T_c compounds

A. Ruydi,^{1,2,3} P. Abbamonte,^{1,4} M. Berciu,⁵ S. Smadici,^{1,4} H. Eisaki,⁶
Y. Fujimaki,⁷ S. Uchida,⁷ M. Rübhausen,³ and G. A. Sawatzky⁵

¹National Synchrotron Light Source, Brookhaven National Laboratory, Upton, NY, 11973-5000, USA

²Materials Science Centre, University of Groningen, 9747 AG Groningen, The Netherlands

³Institut für Angewandte Physik, Universität Hamburg, Jungiusstraße 11, D-20355 Hamburg, Germany

⁴Physics Department and Frederick Seitz Materials Research Laboratory, University of Illinois, Urbana, IL, 61801

⁵Department of Physics and Astronomy, University of British Columbia, Vancouver, B.C., V6T-1Z1, Canada

⁶Nanoelectronics Research Institute, AIST, 1-1-1 Central 2, Umezono, Tsukuba, Ibaraki, 305-8568, Japan

⁷Department of Superconductivity, University of Tokyo, Bunkyo-ku, Tokyo 113, Japan

(Dated: November 12, 2018)

The distribution of holes in $\text{Sr}_{14-x}\text{Ca}_x\text{Cu}_{24}\text{O}_{41}$ (SCCO) is revisited with semi-empirical reanalysis of the x-ray absorption (XAS) data and exact-diagonalized cluster calculations. A new interpretation of the XAS data leads to much larger ladder hole densities than previously suggested. These new hole densities lead to a simple interpretation of the hole crystal (HC) recently reported with $1/3$ and $1/5$ wave vectors along the ladder. Our interpretation is consistent with paired holes in the rung of the ladders. Exact diagonalization results for a minimal model of the doped ladders suggest that the stabilization of spin structures consisting of 4 spins in a square plaquette as a result of resonance valence bond (RVB) physics suppresses the hole crystal with a $1/4$ wave vector.

PACS numbers:

Two years after the discovery of high- T_c cuprates [1], a new phase of Cu-O based systems, $\text{Sr}_{14-x}\text{Ca}_x\text{Cu}_{24}\text{O}_{41}$ (SCCO), was found [2, 3]. SCCO is a layered material with two different types of copper oxide sheets – one with CuO_2 'chains' and one with Cu_2O_3 'ladders' (see Fig. 1a). The sheets are separated by Sr/Ca atoms, and are stacked in an alternating fashion along the b crystallographic direction. They are structurally incommensurate; the ratio of chain and ladder lattice parameters is $c_c/c_L \approx 7/10$. From charge neutrality, the formal valence of Cu is +2.25, resulting in 6 holes per unit cell if counting from a Cu^{2+} state. The substitution of Ca for Sr redistributes the holes between the chains and the ladders allowing for studies as a function of hole density without the influence of strong scattering by charged impurities.

A hole-doped two-leg spin ladder is the minimum needed to obtain superconductivity (SC) [3, 5, 6], although this competes with an insulating 'hole crystal' (HC) phase [5, 7, 8]. SC with $T_c \approx 12$ K has indeed been found by Uehara *et. al* [9] for samples with $x = 13.6$ under hydrostatic pressure > 3 GPa. Recently, the HC phase in the ladders was also discovered by resonant soft x-ray scattering (RSXS) [10, 11]. The HC is observed to have only odd periodicity ($\lambda_{HC} = 5c_L$ for $x = 0$ and $\lambda_{HC} \approx 3c_L$ for $x = 10, 11$ and 12). The competition between the HC and SC phases in the two-leg spin ladder is believed to be similar to that between ordered stripes and SC in doped two-dimensional Mott insulators [12] making it an important model system to try to understand. In fact, a two-dimensional model of coupled two-leg spin ladders [13] was used to explain recent neutron scattering data of two-dimensional cuprates $\text{La}_{15/8}\text{Ba}_{1/8}\text{CuO}_4$ [14].

A serious problem exists however in understanding the periodicity of the HC in the ladders in terms of what was thought to be the correct doped hole density of the

ladders. The often accepted doped hole density of $\delta_L \approx 1/14$ (i.e. ~ 1 hole for every 14 Cu's) in the ladder and $\delta_c \approx 5/10$ (i.e. ~ 5 holes for every 10 Cu's) in the chain is a much too small density to arrive at a HC periodicity of $5c_L$ in ladder units. Until we understand this we really cannot reach any conclusions with regard to proposed models predictions regarding charge and spin ordering in these structures.

The present paper deals with this problem and presents a new interpretation of the polarization dependent x-ray absorption data which leads to a much different charge density distribution between ladders and chains and with which the observed periodicities of hole crystals emerges quite naturally. We conclude that δ_L and δ_c are $2.8/14$ and $3.2/10$ for $x = 0$, respectively, and the number of holes in the ladder increases almost linearly with x , reaching $\delta_L = 4.4/14$ and $\delta_c = 1.6/10$ for $x = 11$. The end result is a strong support of the rung based hole pairing predicted using simple $t-J$ like models [7]. We attribute the absence of the HC with $\lambda = 4c_L$, expected at $x = 4$ but not observed, to simple RVB-physics.

The distribution of holes between the chains and ladders is essential in determining the answer for the problem we mentioned above, and most physical properties. Like in high- T_c cuprates, the holes are expected to enter into O $2p$ orbitals and to form spin compensated local bound states with a Cu $3d$ hole [15] referred to as Zhang-Rice (ZR) singlets [16]. Various experiments suggest that $\delta_L \approx 1/14$ and $\delta_c \approx 5/10$ at $x = 0$, and provide evidence for a transfer of holes from the chains to the ladders upon Ca substitution. X-ray absorption measurements [17] find that δ_L ranges from $0.8/14$ for $x = 0$ to $1.1/14$ for $x = 12$. Optical conductivity data [18] find a range from $1/14$ to $2.8/14$, while ^{63}Cu NMR studies [19] find a range from $1/14$ to $3.5/14$. However, the opti-

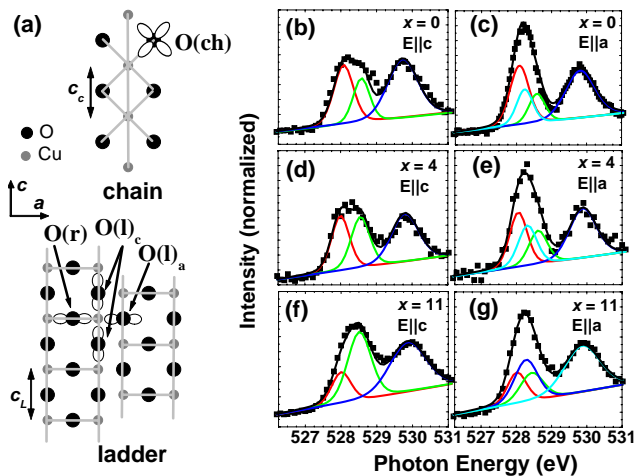


FIG. 1: (a) Structure of chains and ladders. The orientation of the O $2p$ orbitals involved in the ZR singlets are indicated. The three different oxygen sites are identified for the ladder. The right-side panels show XAS for $E||c$ and $E||a$ and its theoretical fits, for $x = 0$ (b,c), $x = 4$ (d,e), and $x = 11$ (f,g). Squares are the experimental data. Black, red, green, cyan and blue lines, are theoretical curve for total fitting, respectively contributions of O(ch), O(l), O(r) and UHB.

cal conductivity and the NMR data analysis at $x = 0$ are based on the neutron diffraction observation [20] of what was thought to be a superlattice reflection corresponding to a chain charge density wave (CDW) consistent with $\delta_c = 5/10$, and thus $\delta_L = 1/14$. More recent neutron studies [4, 21] and analysis of the crystal structure by van Smaalen [22] have clearly shown that this peak is expected in the basic crystal structure and is therefore not evidence for a CDW.

The only direct measurement of the hole density distribution comes from polarization dependent XAS. This is also subject to interpretation, and the model used previously had unexplained discrepancies with regard to the polarization-dependence. In Nücker *et al.*'s analysis [17] of the XAS data it is concluded that the holes are mainly concentrated on the chains. Their interpretation assumes that there are only 2 distinct O $1s$ pre-edge absorption energies, one (H1) corresponding to holes in the chains and the other (H2) to holes in the ladders. The H1 peak should be independent of the ac-plane polarization since the lobes of the O $2p$ orbitals involved in the chain ZR singlets are oriented at 45° to the a - and c -axes (see Fig. 1a). The H2 peak should be strongly polarization dependent since the rung O and the leg O have different hole amplitudes. However, for $x = 0$, XAS data shows that H1 is as strongly polarized as H2. In Ref. [17] it is argued that this effect is small and therefore is neglected.

Single crystals of SCCO were grown by travelling solvent floating zone techniques [24]. The surfaces were prepared in the manner described in Ref. [10]. Polarization-dependent XAS measurements in the fluorescence detection mode were carried out on the soft x-ray undulator line X1B at the National Synchrotron Light Source. The

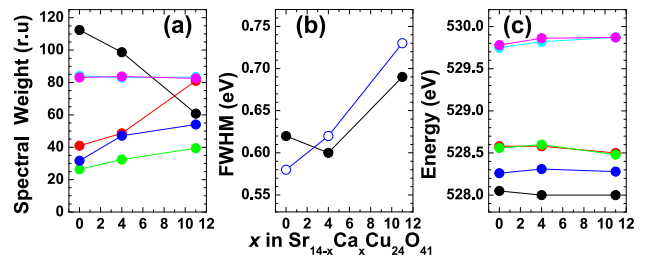


FIG. 2: (a) Spectral weight (SW) (b) full width at half maximum (FWHM) and (c) energy of O(ch) (black), O(l)_c (red), O(l)_a (green), O(r) (blue), UHB for $E||c$ (cyan) and UHB for $E||a$ (magenta) as function of x . Blue open-circles are for oxygen ions in the ladders.

energy resolution in the range of interest was about 200 meV. The spectra were corrected for incident flux variations and were normalized at about 70 eV above and 10 eV below the edge where the absorption is atomic like and structureless.

The $x = 0$ spectrum shown in Fig. 1(b)&(c) is identical to that published in Ref. [17]. Like them, we assign the lowest energy structures to the holes doped in O $2p$ orbitals and the higher energy structure at about 530 eV to transitions to the upper Hubbard band (UHB) or Cu $3d$ orbitals. These are followed by a broader structure due to transitions to unoccupied bands hybridized with O $2p$ and $3p$ states. The UHB structure is only weakly polarization dependent, as expected given the symmetry of the empty $d_{x^2-y^2}$ orbital. Since the point group symmetry for the ladder is not quite D_{4h} (the four O surrounding a Cu are not identical, see Fig. 1a) some polarization-dependence remains. In addition, there is a strongly polarization dependent feature at lower energies, composed of at least two components. In Ref. [17], XAS data for La₃Sr₁₁Cu₂₄O_{41.02} (with only 3 holes per unit cell) shows only one nearly polarization independent structure at the lower energy. As concluded there, this strongly suggests that the holes involved are almost solely on the chains, where all O sites O(ch) are identical, and with $2p$ orbitals oriented to 45° (see Fig. 1a).

In ladders, things are more complicated. There are two types of O sites: the rung sites, O(r), coordinated by 2 Cu ions, and the leg sites, O(l), coordinated by 3 Cu ions (see Fig. 1(a)). The different coordination numbers result in different binding energies for the core $1s$ and valence $2p$ orbitals. Higher values are expected for the orbitals of O(l), while those of O(r) should be close to O(ch) which is also coordinated by 2 Cu ions. Moreover, each ladder ZR singlet involves one O(r)_a, two O(l)_c from the leg, and one O(l)_a from the leg of a neighboring ladder. The subscripts a and c refer to the polarization needed to observe O $1s$ to $2p$ transitions. For a -polarization, transitions are possible for O(r)_a and O(l)_a at different energies, while for c -polarization, transitions are only possible from 2 identical O(l)_c, with energy close to that of O(l)_a.

We performed a simultaneous least-square fit to all the measured spectra. Outputs of the fits, namely the spec-

tral weight (SW), full width at half maximum (FWHM) and various energies are shown in Fig. 2(a)-(c). The number of holes $\delta_L = (3 - 5\delta_c)/7$ are determined from the spectral weights of the various absorption lines:

$$\delta_L = \frac{3(SW_{O(r)_a} + SW_{O(l)_a} + SW_{O(l)_c})}{7(SW_{O(r)_a} + SW_{O(l)_a} + SW_{O(l)_c} + SW_{O(ch)})} \quad (1)$$

where $SW_{O(ch)}$ is the total SW for both polarizations.

We start with $x = 0$. XAS data and theoretical fits are shown in Figs. 1(b),1(c). For $E||c$, the doped hole region has at least two structures. In our interpretation this is due to the energy difference between $O(ch)$ and $O(l)_c$. For $E||a$, the contribution of $O(l)_c$ should be replaced with that of $O(l)_a$ and $O(r)_a$, thus shifting more weight to the lower energy. This is indeed consistent with the data. In our fitting results, shown in Fig. 2, the energy of $O(r)_a$ is about 0.2 eV higher than that of $O(ch)$, while the energy of $O(l)_c$ and $O(l)_a$ are roughly equal and about 0.5 eV higher than that of $O(ch)$. The SW of the UHB is almost polarization independent. This shows that the ladder holes are distributed nearly isotropically amongst the 4 O involved in the ZR singlet, even though the symmetry is not the full D_{4h} . (If large deviations were found, the ZR picture would not be valid for the ladder holes). The FWHM of $O(ch)$, which is about 0.62 eV, is about 5% larger than the ones in the ladders. From Eq. (1), we find $\delta_L = 2.8/14$ and $\delta_c = 3.2/10$.

We continue the analysis for $x = 4$. In Figs. 1(d),1(e) we show the fitting for $E||c$ and $E||a$ data, respectively. Again, the SW in the UHB is almost polarization independent (Fig. 2(a)) while the energies of the various O sites are close to the $x = 0$ values (Fig. 2(c)), consistent with our understanding of the polarization dependent XAS. From Eq. (1) we find $\delta_L = 3.4/14$ and $\delta_c = 2.6/10$.

Figs. 1(f) and 1(g) show our XAS data for $x = 11$. (The maximum HC intensity occurs at $x = 11$ where the wave vector is closest to $3c_L$ [11]). In Ref. [17] it is claimed that here, the UHB is strongly polarization dependent while the O doped hole pre-edge region is almost polarization independent. Our results show an opposite behavior, like for samples with smaller x . In fact, the shape and the intensity of the hole-doped and UHB peaks of Ref. [17] are similar to ours, and can be made to coincide by rescaling. We conclude that the difference is due to the method used in the normalization of the data.

The fit of the polarization dependent XAS for $x = 11$ is more difficult than for $x = 0$ or 4. The problem is not statistical noise, but rather the structural peaks themselves. We see in Fig. 1(f) & (g) that there is no clear evidence for multiple peaks in the doped hole regime because the energy resolution is too poor to resolve the peaks. We therefore use the $x = 0$ results as input for the fitting. The fits are shown in Figs. 1(f), 1(g). As before, we find that the SW of UHB is almost polarization independent and the energies of the various O sites remain close to the $x = 0$ values (see Fig 2), validating our interpretation. We find $\delta_L = 4.4/14$ and $\delta_c = 1.6/10$. It is important to

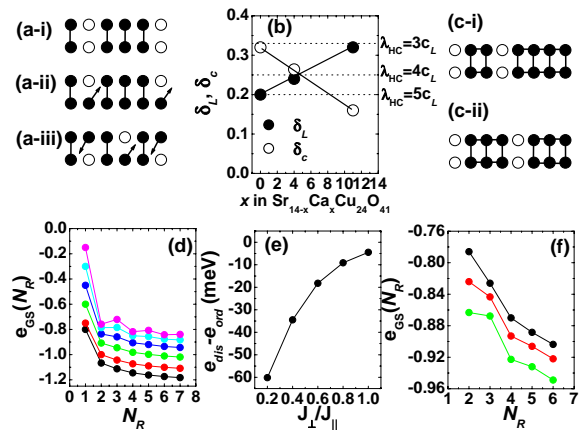


FIG. 3: (a-i)-(a-iii) Scenarios for the ladder hole distribution in a HC with $\lambda = 4c_L$, as predicted by DMRG. Filled (open) circles represent electrons (holes). Arrows indicate the spin of unpaired electrons. (b) The estimated number of holes in the ladders (filled circles) and the chain (open circles). Dashed lines show the number of holes for scenario (a-i), for $\lambda_{HC}/c_L = 3, 4$, and 5. (c-i) Disordered and (c-ii) ordered hole arrangement corresponding to $\lambda_{HC} = 4c_L$. The disordered state has equal numbers of 2-rung and 4-rung spin plaquettes. (d) GS energy per rung, in units of $J_{||}$, as a function of the number of rungs in the spin plaquette. Black, red, green, blue, cyan, and magenta-filled circles are results for $J_{\perp}/J_{||} = 1.2, 1.0, 0.8, 0.6, 0.4$ and 0.2 , respectively. (e) $e_{dis} - e_{ord}$ as a function of $J_{\perp}/J_{||}$, for $J_{||} = 130$ meV (see text for details). (f) $e_{GS}(N_R)$ vs. N_R for $J_{\perp}/J_{||} = 0.4$ and $J_{ring}/J_{||} = -0.1, 0$, and 0.1 (black, red and green-filled circles, respectively).

mention that these results depend strongly on the energy of $O(ch)$. For example, varying it by 0.05 eV changes δ_L by about 0.5/14. This is due to an instability in the fitting process caused by the close proximity of peaks in the pre-edge region (the energy of $O(ch)$ falls close to the leading edge of the hole-doped peak). This is why the $x = 0$ spectrum provides an important reference.

We now analyze some possible scenarios of the hole distribution in the ladder, for these new n_L values. We also consider the connection to the wavelengths $\lambda_{HC} = 3c_L$ ($x = 11$) and $5c_L$ ($x = 0$) of the recently discovered HC [10, 11]. First, DMRG calculations for a single ladder [7] found that holes prefer to pair along the rungs, resulting in a charge density wave shown pictorially in Fig. 3 (a-i). For periodicity $\lambda_{HC} = Nc_L$, the doped hole density in ladder δ_L should be $1/N$, i.e. $\delta_L = 0.2$ if $N = 5$, $\delta_L = 0.25$ if $N = 4$ and $\delta_L = 0.333$ if $N = 3$. These values are very close to our new XAS estimates, as shown in Fig. 3(b). Surprisingly, however, the $\lambda_{HC} = 4c_L$ HC, which is predicted by DMRG [7, 8] to be a stable phase, is not observed in RXS [11]. While the study of this discrepancy is on going, a possible explanation is proposed below. Another hole distribution consistent with these λ_{HC} values, not involving pairing, and also discussed in Ref. [7], is single rung bond-centered holes which is shown in Fig. 3(a-ii). Since δ_L for this case is halved, this model does not match our XAS results. In

a third scenario proposed in Ref. [7], the holes could be site centered, alternating between the two legs as shown in Fig. 3(a-iii). While this matches the δ_L values, it requires an odd number of undoped rungs in the HC unit cell and is therefore inconsistent with the observed $N = 3$ and $N = 5$ HC. We conclude that our results support the scenario of holes paired along the rungs.

Assuming rung-paired holes, a minimal model of the doped ladder is an antiferromagnetic Heisenberg Hamiltonian plus a cyclic four spin exchange term [26, 27]:

$$\mathcal{H} = J_{\parallel} \sum_{\substack{n=1 \\ \alpha=1,2}}^{N_R-1} \mathbf{S}_{\alpha,n} \cdot \mathbf{S}_{\alpha,n+1} + J_{\perp} \sum_{n=1}^{N_R} \mathbf{S}_{1,n} \cdot \mathbf{S}_{2,n} + \mathcal{H}_{\text{ring}}$$

Here, $N_R = N - 1$ is the number of undoped rungs per HC unit cell, $\alpha = 1, 2$ indexes spins on the two legs, and J_{\perp} and J_{\parallel} are exchange couplings along the rung and leg, respectively. We assume no coupling between spins on opposite sides of rungs occupied by paired holes. $\mathcal{H}_{\text{ring}} = J_{\text{ring}} \sum_{n=1}^{N_R-1} \{ \frac{1}{4} + \mathbf{S}_{1,n} \cdot \mathbf{S}_{1,n+1} + \mathbf{S}_{2,n} \cdot \mathbf{S}_{2,n+1} + \mathbf{S}_{1,n} \cdot \mathbf{S}_{2,n+1} + \mathbf{S}_{2,n} \cdot \mathbf{S}_{1,n+1} + \mathbf{S}_{1,n} \cdot \mathbf{S}_{2,n} + \mathbf{S}_{1,n+1} \cdot \mathbf{S}_{2,n+1} + 4\{(\mathbf{S}_{1,n} \cdot \mathbf{S}_{2,n})(\mathbf{S}_{1,n+1} \cdot \mathbf{S}_{2,n+1}) + (\mathbf{S}_{1,n} \cdot \mathbf{S}_{1,n+1})(\mathbf{S}_{2,n} \cdot \mathbf{S}_{2,n+1}) - (\mathbf{S}_{1,n} \cdot \mathbf{S}_{2,n+1})(\mathbf{S}_{2,n} \cdot \mathbf{S}_{1,n+1})\} \}$ is a four-spin cyclic exchange.

We use exact diagonalization to find the ground state for various N_R values. The ground-state (GS) energy per rung, $e_{GS}(N_R) = E_{GS}(N_R)/N_R$, is shown in Fig. 3 (d) for various ratios of J_{\perp}/J_{\parallel} and $J_{\text{ring}}=0$. The value of J_{\perp}/J_{\parallel} is not known accurately, but is believed to be between 0.5 and 1.13 [19, 29, 30, 31, 32, 33]. An even/odd oscillation is observed for small N_R and $J_{\perp}/J_{\parallel} < 1$, favoring $N_R = 2$ and 4 ($\lambda_{HC} = 3, 5c_L$). The origin of this oscillation is simple. The limit $J_{\parallel} \gg J_{\perp}$ corresponds to two AFM chains weakly coupled along the rungs. For even N_R , spins on each leg pair in a RVB-like state, and E_{GS} is low. For odd N_R , each leg has an unpaired spin, significantly increasing E_{GS} . In the limit $J_{\perp} \gg J_{\parallel}$, the GS consists of spin-singlets along the rungs and the parity of N_R is irrelevant. At large N_R , e_{GS} converges to the

bulk value. This even/odd oscillation provides a possible explanation for the absence of a HC with $N_R = 3$ ($\lambda_{HC} = 4c_L$). This HC costs an energy $e_{\text{ord}} = 6e_{GS}(3)$ per two unit cells (see Fig. 3(c-ii)). A disordered phase, at the same doping, has equal numbers of $N_R = 2$ and $N_R = 4$ plaquettes and an energy $e_{\text{dis}} = 2e_{GS}(2) + 4e_{GS}(4)$ for the same length (see Fig. 3(c-i)). If $e_{\text{dis}} < e_{\text{ord}}$, the HC phase is unstable. For $J_{\parallel} = 130$ meV, we plot $e_{\text{dis}} - e_{\text{ord}}$ in Fig. 3(e), showing that the disordered phase is energetically favorable, especially for lower values of J_{\perp}/J_{\parallel} .

We have also studied the effect of $\mathcal{H}_{\text{ring}}$ on E_{GS} . Such terms appear in 4th order perturbation expansions in the strong coupling limit of the Hubbard model [26] and are known to play an important role for Wigner crystals and ³He solid. Typical results for $e_{GS}(N_R)$ are shown in Fig. 3(f), for $J_{\perp}/J_{\parallel} = 0.56$ [28] and $J_{\text{ring}}/J_{\parallel} = -0.1, 0$, and 0.1. Since the sign of the ring exchange and superexchange should be the same [26], it follows that a large J_{ring} suppresses the even-odd effect. For example, for $J_{\perp}/J_{\parallel} = 0.56$, $e_{\text{dis}} - e_{\text{ord}}$ increases from -20.8 meV if $J_{\text{ring}} = 0$, to -12.5 meV if $J_{\text{ring}}/J_{\parallel} = 0.1$. We conclude that for reasonable values of J_{\perp} , J_{\parallel} and J_{ring} this simple model offers a possible explanation for the absence of the $\lambda_{HC} \sim 4c_L$ HC. An accurate determination of the exchange couplings is needed before the issue can be settled.

In conclusion, we propose a new interpretation of polarization dependent XAS for SCCO. Based on our analysis combining the XAS and RSXS data, we find strong support for a pairing of holes in the rungs of the ladders. We also give a possible explanation for the absence of the HC with 1/4 periodicity in terms of RVB physics.

We acknowledge helpful discussions with I. Affleck, A. Sandvik, G. Blumberg and J. Zaanen. This work was supported by FOM, US Department of Energy, Canadian funding agencies: NSERC, CIAR, and CFI, the 21st Century COE program of the Japan Society for Promotion of Science, and the Helmholtz Association contract VH-FZ-007.

-
- [1] J. G. Bednorz and K. A. Müller, Z. Phys. B 64, 189 (1986)
 - [2] E. M. McCarron *et al.*, Mater. Res. Bull. 23, 1355 (1988)
 - [3] T. Siegrist *et al.*, Mater. Res. Bull. 23, 1429 (1988)
 - [4] J. Etrillard *et al.*, Physica C 403, 290296 (2004)
 - [5] E. Dagotto *et al.*, Phys. Rev. B, 45, 5744 (1992)
 - [6] E. Dagotto and T. M. Rice, Science, 271, 618 (1996)
 - [7] S.R. White *et al.*, Phys. Rev. B 65, 165122 (2002)
 - [8] S. T. Carr *et al.*, Phys. Rev. B 65, 195121 (2002)
 - [9] M. Uehara *et al.*, J. Phys. Soc. Jpn 65, 27642767 (1996)
 - [10] P. Abbamonte *et al.*, Nature 431, 1078 (2004)
 - [11] A. Rusydi *et al.*, condmat/0511524 (2005)
 - [12] J. M. Tranquada *et al.*, Phys. Rev. Lett. 78, 338 (1997)
 - [13] G.S. Uhrig *et al.*, Phys. Rev. Lett. 93, 267003 (2004)
 - [14] J. M. Tranquada *et al.*, Nature (London) 429, 534 (2004)
 - [15] H. Eskes *et al.*, Phys. Rev. Lett. 61, 1415 (1988)
 - [16] F.C. Zhang and T.M. Rice, Phys. Rev. B 37, 3759 (1988)
 - [17] N. Nücker *et al.*, Phys. Rev. B, 62, 14384-14392 (2000)
 - [18] T. Osafune *et al.*, Phys. Rev. Lett. 78, 1980-1983 (1997)
 - [19] K. Magishi *et al.*, Phys. Rev. B 57, 11533 (1998)
 - [20] M. Matsuda *et al.*, Phys. Rev. B 54, 12 199 (1996)
 - [21] M. Braden *et al.*, Phys. Rev. B 69, 214426 (2004)
 - [22] S. van Smaalen, Phys. Rev. B 67, 026101 (2003)
 - [23] J. B. Goodenough, Phys. Rev. 100, 564 (1955)
 - [24] N. Motoyama *et al.*, Phys. Rev. B, 55, R3386 (1997)
 - [25] J. J. Yeh *et al.*, At. Data Nucl. Data Tables 32, 1 (1985)
 - [26] M. Takahashi, J. Phys. C: Solid State Phys. 10, 1289 (1977)
 - [27] S. Brehmer *et al.*, Phys. Rev. B 60, 329 (1999)
 - [28] R. S. Eccleston *et al.*, Phys. Rev. Lett. 81, 1702 (1998)
 - [29] T. Imai *et al.*, Phys. Rev. Lett. 81, 220 (1998)
 - [30] K.I. Kumagai *et al.*, Phys. Rev. Lett. 78, 1992 (1997)
 - [31] P. Carretta *et al.*, Phys. Rev. B 56, 14 587 (1997)
 - [32] M. Takigawa *et al.*, Phys. Rev. B 57, 1124 (1998)
 - [33] A. Gozar *et al.*, Phys. Rev. Lett. 87, 197202 (2001)